CORE
Metadata, citation and similar papers at core.ac.uk
Provided by Plymouth Electronic Archive and Research Library

Low dimensional nano-patterned material fabricated by direct-write UV-chemically induced geometric inscription technique

T. ALLSOP,[1,5] R. NEAL,[2] V. KUNDRAT,[1] C. WANG,[1] C. MOU,[3] P. CULVERHOUSE,[2] J. D. ANIA- CASTANON,[5] K. KALLI,[4] D. J. WEBB,[1]

[1]*Aston Institute of Photonic Technologies, Aston University, Aston Triangle, Birmingham B47ET, UK*
[2]*School of Computing and Mathematics, Faculty of Science and Technology, University of Plymouth, Plymouth, PL4 8AA, U.K.*
[3]*Key Laboratory of Special Fiber Optics and Optical Access Network, Shanghai University, Shanghai, 200072, China*
[4]*Nanophotonics Research Laboratory, Department of Electrical Engineering, Computer Engineering and Informatics, Cyprus University of Technology, 31 Archbishop Kyprianos, Lemessos 3036, Cyprus*
[5]*Non-linear Dynamics and Fiber Optics, Instituto de Óptica "Daza de Valdés" (IO-CSIC), Calle de Serrano, 121, 28006 Madrid, Spain*
**Corresponding author: tomallsop@io.cfmac.csic.es or t.d.p.allsop@aston.ac.uk*

Received XX Month XXXX; revised XX Month, XXXX; accepted XX Month XXXX; posted XX Month XXXX (Doc. ID XXXXX); published XX Month XXXX

We have fabricated multi-layered thin films consisting of germanium/silicon each layer have a few tens of nanometres thickness on a planar substrate and using focused 244nm ultra-violet light and optomechnical apparatus normally associated with the inscription of fibre gratings creating controlled microscale and nanoscale planar surface structures. The mechanism is based upon the well-known interaction of germanium oxides and ultra-violet and utilising the spatial and structural alteration part of the mechanism. We investigate the process that creates these surface topological features that arrange is size of ~100 nm to ~10μm along with the creation of sub-micron periodic structures; 500nm. Using a metal overlay in conjunction the multi-layered thin film generates arrays of metal nano-antennae with a mean radius of 130nm and typical length of 20μm with a period of 0.5μm, typical array length of 2cm. Furthermore, each nano-antenna consists of "nano-blocks" this fine structure yields a large spectral tunability range in excess of 1μm. **© 2018 Optical Society of America**

http://dx.doi.org/10.1364/OL.99.099999

The creation of surface features conventionally comes under the general topic heading of photolithography and is important various areas of technology and science. UV photolithography is an important in the electronics/printed circuits and employed on an industrial scale [1, 2]. This area of technology has been improving with the advent of UV-Nanoimprint Lithography, UVNL [3, 4], extreme ultraviolet (EUV) lithography [5] and Laser Interference Lithography LIL [6]. The motivation for the development of the UVNL, EUV and LIL is the production of cost effective lithographic patterning with high accuracy for integrated circuity along with the possibilities of new nano-scale devices for new applications in a variety of different disciplines of science and technology. There are a myriad of publications within the technical field lithography to be used in differing areas of technology [6] but of particular relevance to this work is the application of photolithography in the fabrication of devices that utilises surface plasmons for sensing applications with particular interest in biosensors [4, 7, 8]. These aforementioned sensors have many differing surface topologies and sizes to generate surface plasmons, for example holes and table/discs [9, 10].

The common factor between all of the fabrication techniques and the resultant sensors is that the procedures in fabrication are lengthy and complex; involving many stages to reach the final product. This can be seen by looking the procedures of UVNL, EUV and LIL they use still a photo-resist material and multiple stage processing, such as, mechanical imprinting, the spinning of photo-resist, UV exposure, etching techniques along with using wet chemistry procedures [3-10].

The fabrication procedure that we are using is based upon the spatial structural changes of germanium brought about by its interaction with 244nm UV laser light, a physical phenomenon that is used to produce grating devices in optical fibre [11] and is investigated using planar samples [12]. This process doesn't use etching, wet chemistry or photoresist in the fabrication process, thus reducing the complexity of fabrication. This technique is illustrated by using a focused 244nm UV laser working in conjunction with a phase mask in the fabrication of uniform corrugations on germanium surface on the nanometre scale. Also using focused UV laser to produced concentric circles on the

micrometre scale. Furthermore, the germanium layer is has additional over-layers consisting of silicon dioxide and a metal (gold or platinum), using these coatings with the technique described here produces arrays of nanowires which as supported by the silicon dioxide. The size of the surface topological features that arrange is size of ~100 nm to ~10μm along with the creation of sub-micron periodic structures; 500nm which are repeatable structures with a total length in excess of 2cm. Thus creating what is communally called a nano-antenna arrays which are used as optical sensing platform for biosensors and chemical sensors.

The interaction of the germanium and the 244nm UV light was investigated, a thin film coating of germanium with a thickness of 48nm was deposited upon a BK7 glass substrate which had a thickness of 150μm. The reasoning for using a thickness of 48nm of germanium comes from some previous work [13]. The thin film of germanium and other thin film were deposited using an RF sputtering machine (Nordico 6 inch RF/DC 3 target excitation machine, Nordiko 6, Nordiko Technical Services Limited, Havant, Hampshire, UK). These germanium coated planar substrates are then mounted and spatially aligned to be exposed to various intensities of 244nm, opto-mechanical arrangement of the apparatus is the same for the UV inscription of optical fibre gratings [11]. The UV beam was implicated by three configurations. One, single axis focused along the line of travel of the air-bearing stage (using a plano-convex lens focal length of 80mm) then passed through a phase mask (period of 1.018 μm). Two, focus the beam in two axis parallel and perpendicular to line of travel of the air-bearing stage (using two plano-convex lens both having focal lengths of 80mm). Three combining both the phase mask and configuration two, see figure 1.

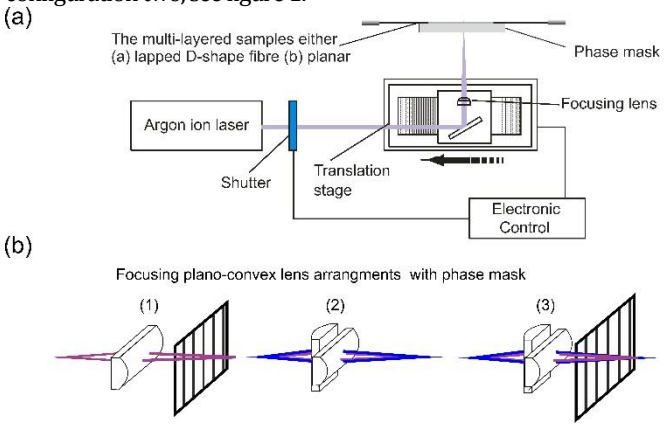

Fig. 1. (a) Schematic of opto-mechanical apparatus for the creation of the surface structures on planar and fibre substrates. (b) spatial focusing arrangement of the plano-convex lenses and the phase mask

A series of experiments where conducted on germanium coating (thickness of 48nm) on planar substrate using various inscription powers from 100mW to 180mW of 244nm UV laser light (Argon Ion laser, Sabre Fred Coherent Inc) and using a constant scan velocity of 0.1m/s for the three focusing arrangements shown in figure 1b. Using configuration one (phase and single lens) produced two main surface features, a fine nanoscale corrugation with the amplitude is related to the irradiance subjected to the sample and a secondary background feature with greater physical height, example shown in figure 2a and 2b. Figure 2a shows the overall diffraction pattern produced by the phase mask with predominant periods ~18μm, whilst figure 2b shows the interference pattern produced from the overlapping fringes, with the predominant periods in the range of 0.5μm to 1.1μm. The relationship between the size of the surface feature and irradiance depends upon the optical configurations, for example, using configuration two there appears to saturation occurring at the lower energies used, creating features with heights of 0.6μm. The fine surface structure period varied with irradiance for the given phase mask used. These results are summarised in figures 3a to 3d, the inspection of the fine structure (interference) results are shown in figure 3a and 3c. General observation for these results is the increasing of the irradiance seems to increase the number of smaller periods and appears to have a saturation effect occurring with a surface corrugation amplitude reaching 7 to 10nm, figure 3c. This saturation effect is understandable to the fact that there is only a limited amount of germanium present within the coating, and secondly as the irradiance increases the average absorption of UV per unit area increases over an average fringe oscillation. Therefore, the maximum amplitude in the background spatial perturbation will decrease, which can be seem in figure 3d

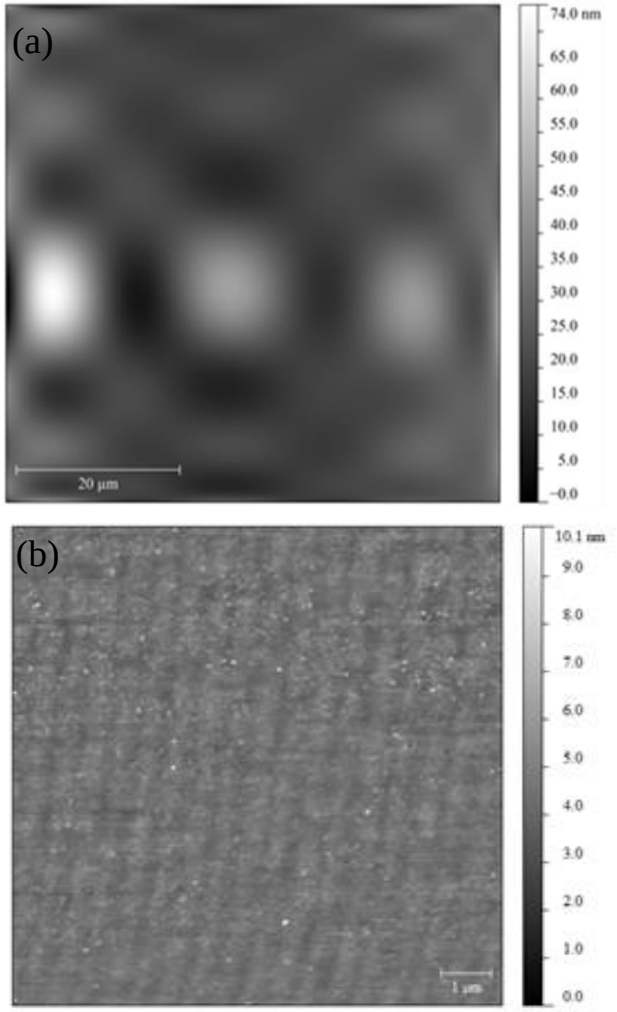

Fig. 2. The variation of the surface topology of a germanium coating (thickness 48nm) on a planar substrate obtained from the 244nm UV (power 180mW and scan velocity of 0.1 mm/s) light through a phase mask (period of 1.018 μm). (a) The irradiance diffraction pattern of at approximately 40μm out of focus. (b) The finer interference pattern produced by diffracted beams.

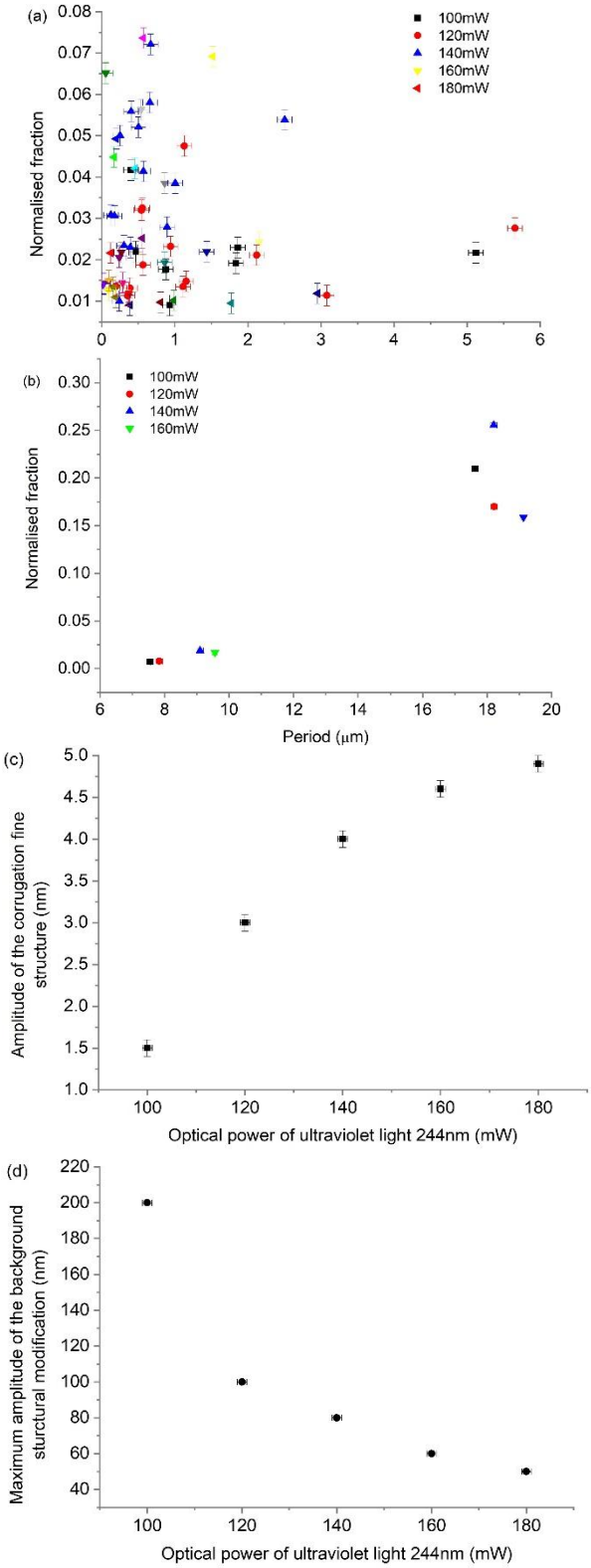

Fig. 3. Spatial characteristics of the UV light irradiated germanium coating (thickness 48nm) planar samples. (a) Periods of the fine corrugation produced from the interference pattern of the UV light. (b) Periods of the background spatial perturbation produced by the diffraction pattern. (c) Amplitude of the fine corrugations. (d) Maximum height of the background spatial perturbation.

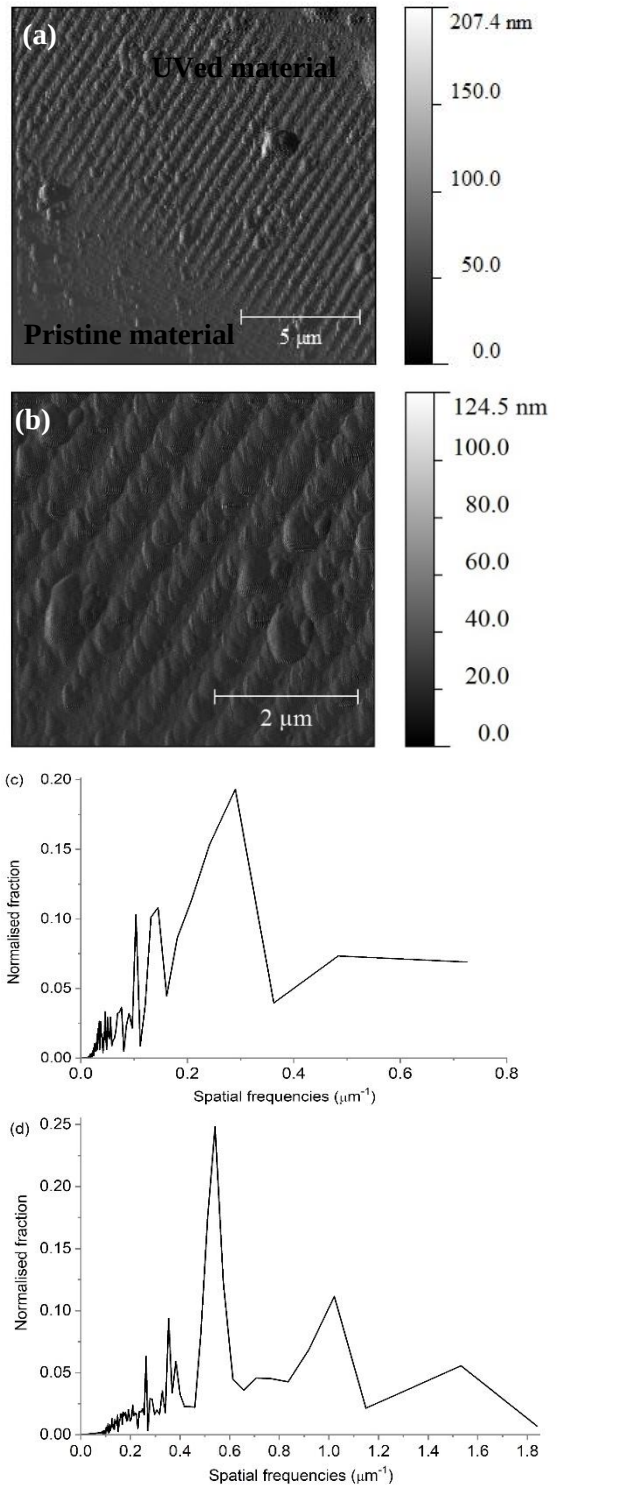

Fig. 4. The surface corrugation of a multi-layered coating (germanium 48nm, silicon dioxide 48nm, and gold 32nm) on a planar substrate (a) An AFM scan showing regions of pristine coating with no UV light exposure and exposed regions with nano-structuring. (b) An AFM scan showing the secondary detail of the topology associated with each of the individual nano-antenna. (c) and (d) typical abundance and variation of the spatial frequencies along an individual nano-antenna and across the nano-antennas respectively.

Following this initial set of experiments additional layer where deposited upon the germanium, a layer of silicon dioxide (thickness of 48nm) followed by metal film of either gold (thickness of 32nm), silver (thickness 32nm) or platinum (thickness of 36nm), these thicknesses where chosen from modelling procedure describe in REF 14. AFM scans of one example of metal is shown in figure 4 with a gold metal overlay and along with an unexposed region of the multi-layered coating where there is no surface corrugation see figure 4a. The resultant height of the corrugation varied with the overlay metal, typically for silver yielded ~110nm with gold yielding a slight less height of ~70nm and platinum producing the smallest heights of ~40nm. The reasons for this height variation with differing metals is probably two-fold, one the skin depth; $d_s=\lambda/4\pi\kappa$ where λ is wavelength and κ is attenuation index [14]. The skin depth values for silver at 244nm is ~35nm compared to gold that has a value of ~13nm and platinum a value of ~10nm thus the higher intensity of the UV irradiance reaches the germanium, therefore there is a greater reaction with germanium and higher compaction occurs yielding the highest amplitude of the corrugation. Also considering that the melt-point for silver, 961.8 ^{0}C is the lowest along with having greatest thermal conductivity; 429 $Wm^{-1}k^{-1}$ [13] which helps to transfer the generated thermal energy to the germanium region and thus making the material more malleable. The inclusion of a metal overlay in the sputtering procedure creates an array of nano-antennae during the UV exposure.

Furthermore, on a finer resolution AFM scan of the UV processed regions shows structure within a single nano-antenna figure 4b. Fast Fourier analysis (FFT) was performed the single profiles of individual nano-antenna and on cross-sections between nano-antennas, figures 4c and figure 4d respectively. The FFT revealed a predominant period is 0.54 μm and 1.02 μm across the corrugations which is expected because the fundamental period of the phase mask is $1\mu m^{-1}$, figures 4c and 4d. Secondly, the fundamental period within an individual antenna is 0.29μm with possibly be explained by the fact the phase mask generates fringe pattern in three-dimensions plus the pattern are being focused upon the planar sample thus producing a bead-like pattern associated with the germanium that is exposed highest intensity of the UV light, see figure 4b.

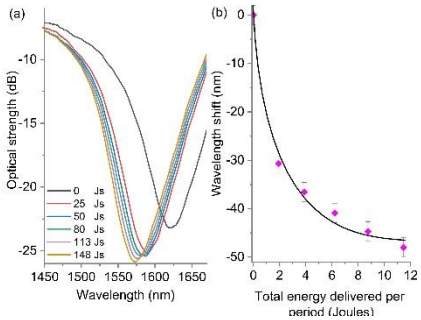

Fig. 5. (a) The spectral behavior a the fibre device with a platinum (36nm) metal as a function UV dosage (a) the transmission spectrums (b) the wavelength shift the central resonance of the plasmon.

These structures can create surface plasmons when illuminated with polarized light and are the subject of research at the moment by the authors [13-15]. During the fabrication procedure, using multi-exposures to UV irradiance the observed surface plasmon resonance (SPR) shifts, this spectral behaviour is expected due to the fact the surface plasmons resonance depends on the size and shape of the nano-antennae supporting the surface plasmon [9, 10]. This SPR wavelength shift with UV dosage exposure is shown in in figure 5; the shifting SPR in the transmission spectra and the overall spectral response. Inspecting figure 5b the increase in UV dosage is a decreasing effect on altering SPR spectral location, this is consent with the results obtained for the germanium layer and examples shown in figure 3.

In conclusion, the presented work shows that this simple procedure as a flexibility to create complex structures not show by other inexpensive fabrication methods, secondly, that it has the potential to create repeatable structures over on the centimeter scale. Thirdly, this inexpensive fabrication method as the potential to create low dimensional nanostructured materials for such applications as nanoplasmonics

Funding. UK Engineering and Physical Sciences Research Council (EP/J010413), UK Engineering and Physical Sciences Research Council (EP/J010391)

Acknowledgment. Each of the authors contributed as following: T. A. developed the original concept. T.A. modelled, designed and performed experiments, analysed the experimental data. T.A., C.M., R.N., fabricated and UV processed the test samples. Characterisation of materials and performed experiments V. K. T. A., K.K. The manuscript was written by T.A., C. M., K.K., D.J.W., R. N. and P.C. All authors discussed the results and commented on the manuscript.

References

1. S. Roth, L. Dellmann, G. A. Racine, N. F. De Rooij. Jn. Micromechanics and Microengineering, **9**, no. 2, 105, (1999).
2. D. J. Resnick, W. J. Dauksher, D. Mancini, K. J. Nordquist, T. C. Bailey, S. Johnson, N. Stacey et al. Journal of Vacuum Science & Technology B: Microelectronics and Nanometer Structures Processing, Measurement, and Phenomena **21**, no. 6 , 2624-2631, (2003).
3. M. Bender, A. Fuchs, U. Plachetka, H. Kurz. Microelectronic Engineering **83**, no. 4, 827-830, (2006).
4. A. Cattoni, P. Ghenuche, A.-M. Haghiri-Gosnet, D. Decanini, J. Chen, J-L. Pelouard, S. Collin. Nano letters **11**, no. 9, 3557-3563 (2011).
5. B. Päivänranta, A. Langner, E. Kirk, C. David, Y. Ekinci. Nanotechnology **22**, no. 37, 375302, (2011).
6. J-H Seo, J. H. Park, Z. Ma, J. Choi, B-K. Ju. Jn nanoscience and nanotechnology **14.2**, 1521-1532, (2014).
7. J. Anker, P. Hall, O. Lyandres, N. C. Shah, J. Zhao, R. P. Van Duyne. Nature materials **7**, no. 6, 442-453, (2008).
8. Lee, Seung-Woo, Kyeong-Seok Lee, Junhyoung Ahn, Jae-Jong Lee, Min-Gon Kim, and Yong-Beom Shin. ACS nano **5**, no. 2, 897-904 (2011).
9. D. B., Shao, S. C. Chen. Nano letters **6**, no. 10, 2279-2283, (2006).
10. W. Srituravanich, N. Fang, C. Sun, Q. Luo, X. Zhang. Nano letters **4**, no. 6, 1085-1088, (2004).
11. K. Hill, O., B. Malo, F. Bilodeau, D. C. Johnson, J. Albert. Applied Physics Letters **62**, no. 10, 1035-1037, (1993).
12. F. J. Young, J. E. Sipe, H. M. Van Driel. Phys. Review B **30(4)**, 2001, (1984).
13. T. Allsop, R. Neal, C. Mou, K. Kalli, S. Saied, S. Rehman, D. J. Webb, P. F. Culverhouse, J. L. Sullivan, I. Bennion. IEEE Jn of Quantum Electronics **48(3)**, 394-405, (2012).
14. T. Allsop, R. Neal, C. Mou, P. Brown, S. Saied, S. Rehman, K. Kalli et al. Applied optics **48(2),** 276-286, (2009).
15. T. Allsop, Thomas, R. Arif, R. Neal, Ky Kalli, V.Kundrát, A. Rozhin, P. Culverhouse, D. J. Webb. Light: Science & Applications **5(2)**, e16036, (2016).